ORIGINAL ARTICLE

Spatial distribution characteristics of drought disasters in Hunan Province of China from 1644 to 1911 based on EOF and REOF methods

Shuoben Bi[1] · Xiangkai Qiu[2] · Guojie Wang[1] · Yucheng Gong[1] · Luye Wang[1] · Mengya Xu[1]

Abstract
Under the background of climate warming, drought disasters occur frequently in China, especially in the Central China. In this study, drought disaster grade sequences from 14 representative stations were chosen from 268 years of drought disaster historical data for the Hunan Province of China collected during the Qing Dynasty (1644–1911). The empirical orthogonal function (EOF) and rotated empirical orthogonal function (REOF) methods were used to conduct a spatial characteristics analysis of these drought disasters. The results are as follows. (1) There was an inconsistency between the frequency and intensity of the drought disasters. (2) The spatial distribution of the first four EOF loads for the drought disasters showed regional consistency; however, there was a difference in the anti-phase changes in the east–west, south–north, and central directions. (3) The features of the drought disaster distribution in the Hunan Province during the Qing Dynasty are evident, and according to the high values (absolute value ≥ 0.6) for the first six EOF rotational loads, the study area can be divided into the following sections: northeast Xiang (Section I), west Xiang (Section II), southeast Xiang (Section III), middle Xiang (Section IV), north Xiang (Section V), and southwest Xiang (Section VI). The study of drought disasters in Qing Dynasty is of great significance and reference value for disaster prevention, disaster reduction and climate prediction.

Keywords Drought disaster · Spatial characteristics · Qing Dynasty · Hunan Province · Empirical orthogonal function · Rotated empirical orthogonal function

Introduction

Drought is a weather phenomenon characterized by a long-term lack of rain. When the overall precipitation is not enough to support the human population's needs, and results in economic losses and human casualties, the event is called a drought disaster (Wen and Jiang 2007). The main consequences of prolonged periods of low precipitation are a lack of surface water and a decline in groundwater levels. Drought has become the most widespread climate disaster (National Science and Technology Commission 1990).

✉ Shuoben Bi
  bishuoben@163.com

1 School of Geographical Sciences, Nanjing University of Information Science and Technology, No. 219 Ningliu Road, Pukou District, Nanjing 210044, Jiangsu Province, China

2 Institute of History of Science and Technology, Nanjing University of Information Science and Technology, Nanjing, Jiangsu, China

Continued warming of the global climate has led to more droughts and increased drought losses (Xu et al. 2011). In recent years, scholars from around the world have made much progress in the study of droughts. Piervitali and Colacino (2001) used historical literature to establish the drought chronology of the Sicilian region from 1565 to 1915. Findell and Delworth (2010) indicated that warm Pacific and Atlantic Sea Surface Temperature (SST) anomalies can lead to climate reversal and frequent flood, while Ummenhofer et al. (2011) argued that the drought in southeastern Australia is related to the influence of the Indian Ocean Dipole (IOD) and the El Nino Southern Oscillation (ENSO). However, applicable tools and their usefulness are still not sufficiently studied. In the Hunan Province, which is a major grain-producing area in China and has been frequently hit by floods and droughts, relevant research is even more limited (Du et al. 2013). Drought research outside China mainly focuses on analyses based on meteorological observation data, while the study of the timing and causes of droughts during historical periods is less of a focus.

The results obtained by Du et al. (2013) indicated that the upper reaches of the major rivers in the Hunan Province have experienced more dry years than the middle and lower reaches over the past 57 years. Furthermore, the region shows a trend of becoming drier during the spring and autumn seasons and wetter during the summer and winter seasons. Guo et al. (2020) analyzed the temporal and spatial variations of the two basins based on 33 rain-gauge data series from 1960 to 2015 using statistical methods, geographical information system spatial analysis and the Mann–Kendall trend test. Guo et al. (2020) found that El Niño and Southern Oscillation events had significant relationships with negative monthly precipitation anomalies. However, our understanding of long-term climate variations is limited by the shortage of meteorological records. Paleoclimatic proxies can be pursued to extend the meteorological records back for centuries to improve our understanding of climatic conditions (Zhao et al. 2017). Xing and Zhao (2011) pointed out that the frequent occurrence of droughts in the Jinan area during the Ming Dynasty were mainly caused by the apparent decrease in the annual precipitation resulting from the cold and dry climate, and that the El Nino phenomenon played a significant role in increasing the number of the drought disasters in the area. Li et al. (2015) through the consolidation of drought data in the Henan region during the Ming Dynasty found that the droughts were more concentrated during the spring, summer, and autumn, and that the droughts were less severe during the middle and late periods of the dynasty. Yang and Zhang (1994) pointed out that the quasi-periodic changes of Hunan's historical droughts occurred in cycles of 2–3, 18–22, 30–40, and 150–180 years, and the droughts were far reaching and severe.

Zhang et al. (2013) used EOF, REOF and Morlet wavelet analysis methods on modern meteorological observation data to analyze the temporal and spatial variation characteristics of meteorological drought days in the Hunan Province from 1960 to 2009. Their results showed that the spatial distribution of meteorological drought days in Hunan is consistent in the entire region, but there are also differences between south and north, northeast and southwest, with opposite changes. Zhang et al. (2018) analyzed the distribution characteristics of summer and autumn droughts and classified the types of these droughts in Hunan. Based on the calculation and analysis of the variation characteristics of drought and flood during the main flood season in the Hunan Province, Luo and Zhang (2010) analyzed the atmospheric circulation and its relationship with spring-sea surface temperature. Luo et al. (2009) established a drought disaster evaluation model for middle and late rice production in the Hunan Province and provided the drought disaster risk zoning of rice production in the Hunan Province. Mi et al. (2016) analyzed the interannual variation and possible causes of summer drought in western Hunan. Xie and Zhu (2005) analyzed the causes of floods and droughts in the Hunan Province and considered Hunan's special geographical location as one of the most fundamental reasons.

The Hunan Province is one of the most frequently affected drought provinces in the south of China. Known as the "having drought 9 years out of ten" (Zhang et al. 2009), such as "a scene of utter desolation, the river dried up and the well withered, the crops did not yield, no grass grows out," "there were starved bodies on the roads, lie horizontally and vertically" and "people as food." The tragic record is not common. Therefore, this study attempted to analyze the spatial distribution characteristics of the drought disasters in the Hunan Province of China and their climatic zonation from 1644 to 1911 during the Qing Dynasty. Scientifically, it is important to understand the spatial changes in drought disasters to reduce the associated losses and to improve drought disaster prediction and relief efforts. The present study contributes in achieving the United Nations' 2030 Agenda for Sustainable Development to advance the Sustainable Development Goals (SDG 13: Climate actions) (Zhang et al. 2019; Achour and Pourghasemi 2020).

Study area and data sources

Study area

The Hunan Province is located in the transition zone from the Yunnan–Guizhou Plateau to the Jiangnan hills and Nanling to the Jianghan Plain. It is bounded between the 24°38′ and 30°08′ north latitude and 108°47′ and 114°15′ east longitude, with a total area of 2,118,000 square kilometers. The eastern, western, and southern areas are surrounded by mountains and gradually inclined to the northeast and the middle, forming an asymmetrical horseshoe-shaped open landform toward the northeast. It is composed of a plain, basin, hilly land, mountain area, and river lake, which crosses the Yangtze River and Pearl River systems, and experiences a subtropical monsoon climate. The province is mainly a mountainous and hilly landform, of which the mountainous area exceeds 50% of the total area. The Hunan Province has a dense network of rivers, with a total length of 90,000 m, mainly including four rivers, Xiangjiang, Zijiang, Yuanjiang, and Lishui, and their tributaries. The Hunan Province flows from the south to the north along the terrain elevation difference to the Yangtze River and Dongting Lake, forming a relatively complete Dongting Lake system. Dongting Lake is the largest lake in the Hunan Province, and it spans the Hunan and Hubei provinces. As the longest river in the Hunan Province, the Xiangjiang River is also one of the seven tributaries of the Yangtze River (Fig. 1).

Fig. 1 Location map of the study area
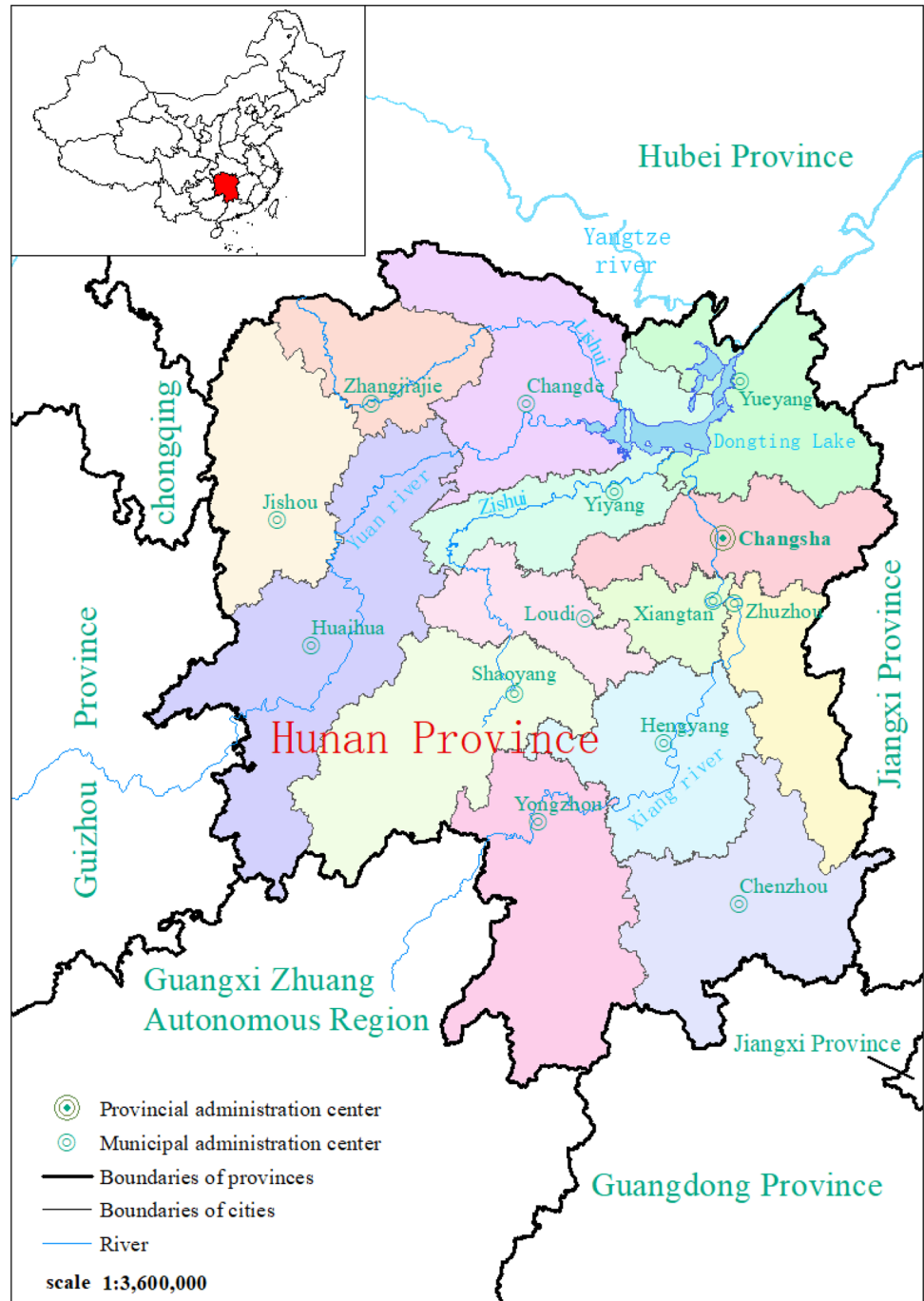
Data sources

The information used in this study was mainly acquired from Zhang Deer's "Three-year Meteorological Records of China" (Zhang 2004), Zeng Qinghua's "China Meteorological Disaster—Hunan Volume" (Wen and Zeng 2006), "Baoqing Fuzhi" (Huang et al. 2009), "Xiangtan County" (Chen and Wang 2010), and other descriptions in local chronicles, and was supplemented by "China Nearly Five Hundred Years of Drought and Drought Distribution Atlas" (Chinese Academy of Meteorological Sciences 1981). This article refers to the "Beijing history of natural disasters" (Yin et al. 1997). According to the description of the droughts in historical drought data, the duration of the recorded drought, the extent of area affected by it, and the damage caused to agriculture and people's way of life affect drought classification. Drought hazards can be divided into three grades (Table 1), with a mild, moderate, and severe drought being classified as grade 1, grade 2, and grade 3, respectively. Years without drought are classified as grade 0.

Table 1 Classifications for drought levels

Grade	Standard	Typical language
Grade 1	The drought spans a single season/is a local drought	Summer no rain, autumn drought, did not rain during the rainy season, spring drought delayed planting rice seedlings, the crops were scorched by the sun for lack of water, plague of locusts, it takes several kilometers to get water
Grade 2	The drought spans two seasons, and affects a large area	Spring and summer drought, the whole area are in disaster, the plant withered, there were starved bodies on the road, the rivers dried-up and the wells withered, a bushel of rice costs one hundred cents, relief
Grade 3	The drought spans three seasons, or is a transboundary drought, causing extensive damage	It did not rain in the three quarter of summer, winter and winter, a scene of utter desolation, there were no crops in the field, people as food, a bushel of rice costs one thousand cents, free of grain this year

Research methods

The EOF (empirical orthogonal function) and the REOF (rotated empirical orthogonal function) are commonly used analytical methods for studying the temporal and spatial characteristics of meteorological variables (Yang and Xu 1994; Shi 2002). It is possible to decompose the meteorological variable field with time and space into linear combinations of spatial patterns and time coefficients that are uncorrelated.

The observation data of a climate variable field can be expressed in the following matrix form:

$$X = \begin{bmatrix} x_{11} & x_{12} & \dots & x_{1n} \\ x_{21} & x_{22} & \dots & x_{2n} \\ & \dots & \dots & \\ x_{m1} & x_{m2} & \dots & x_{mn} \end{bmatrix}, \tag{1}$$

where m is the spatial point, and n is the point in time. xij represents the j-th observed value on the i-th station. The natural orthogonal expansion of the meteorological time series means that Eq. (1) is decomposed into two parts, the space function V and the time function T:

$$X = VT, \tag{2}$$

or

$$x_{it} = \sum_{k=1}^{P} v_{ik}t_{kj} = v_{i1}t_{1j} + v_{i2}t_{2j} \dots + v_{im}t_{mj},$$
$$i = 1, 2, m; t = 1, 2, \dots, n; k = 1, 2, \dots \tag{3}$$

Here, the j-th climate observation on the i-th lattice can be thought of as a linear combination of p v_{ik} and the time function t_{kj}.

The EOF can maximize the variability structure of the whole region of the climate factor field, but it is not conducive for highlighting the local correlation structure and the identification factor distribution type. The REOF is the orthogonal rotation of the original matrix based on the EOF decomposition (large variance rotation), such that the high load vector is concentrated over a few variables, and the rest of the regions are close to 0. Thus, the post-rotation feature field is more stable in time, the spatial distribution structure is simpler and clearer, and it also highlights the abnormal distribution of local features (Chen et al. 2010). Therefore, this study used the EOF and REOF statistical analysis methods to explore the temporal and spatial evolution of drought disaster grades in the Hunan Province during the Qing Dynasty, focusing on the spatial distribution and the distribution of the drought disaster grades in the province to provide the basis for internal zoning predictions.

Results and analysis

Frequency of drought disasters in the Hunan Province during the Qing Dynasty

Statistics on the frequency of drought disasters from 14 sites in the Hunan Province (1644–1911), and the plot of the frequency distribution of the drought disasters (Fig. 2A), are shown in Fig. 2. The sizes of the circles denote the frequency of occurrence; the greater the radius, the higher the number of drought disasters. Drought disasters in the Hunan Province occurred 66.21 times/station during the 268 years under study. The largest number of drought disasters occurred in the Yongzhou, with a frequency of 101, that is, drought disasters occurred during 101 years of the 268 years studied, with an incidence rate of 37.69%, at an average of every 2.65 years. The lowest frequency of drought disasters occurred in Zhangjiajie (only 31), an incidence of 11.57%, with one occurring every 8.65 years. Besides Zhangjiajie, the drought disaster frequency of Xiangxi and Huaihua exceeded 50. It can therefore be observed that drought disasters in the Hunan Province during the Qing Dynasty were more frequent and more serious.

Since the frequency of drought disasters can only reflect the degree of droughts in the region and not the intensity, the weighted average method was used to estimate the average
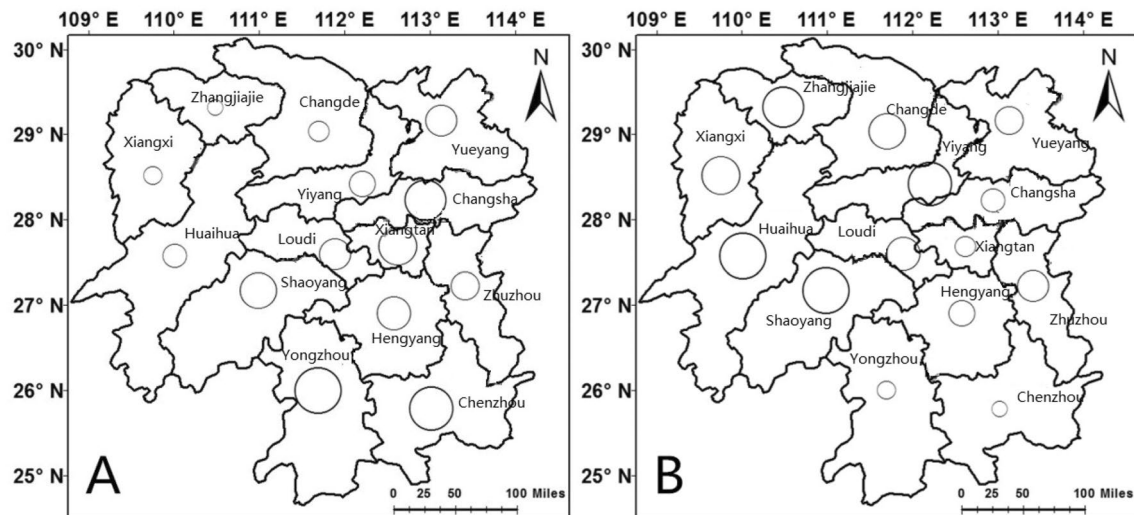
Fig. 2 Spatial distribution of frequency (**A**), and intensity (**B**) of droughts in the Hunan Province during the Qing Dynasty

drought intensity for each site level (*I*) (Gao and Zou 2013) using the following formula:

$$I = (a + 2b + 3c)/(a + b + c), \qquad (4)$$

Here, *I* represents the average drought intensity for site, *a*, *b*, and *c*, with a drought disaster frequency of 1, 2, and 3, respectively.

Figure 2B shows the distribution of drought intensity for 14 sites in the Hunan Province during the Qing Dynasty. As shown in Fig. 2B, the drought intensities for Zhangjiajie and Shaoyang were the largest, and the intensity of the drought disasters was above 1.7. The drought intensities for Chenzhou and Yongzhou were relatively low. Comparing Figs. 2A and B shows that there is no consistency between drought frequency and drought intensity in the Hunan during the Qing Dynasty. A higher number of drought disasters occurred in Yongzhou, Chenzhou, and Changsha. However, the intensities of these occurrences were low. Although Zhangjiajie, Xiangxi, and Huaihua recorded fewer droughts, they were more serious. In addition, Shaoyang and other sites were not only prone to drought disasters, but they also tended to be more serious.

Differences to drought resistance resulted from the varied terrain, landform, soil, vegetation, and other features, including variations in site climate. Obvious regional differences are thus observable. The vegetation coverage in western Hunan is high, and the frequency of drought is low; however, the prominent geological layer is limestone, which has poor soil water retention. The Dongting Lake and the southern Hunan Province are subject to the warm winds of a humid airflow, which resulted in dry heat periods (Liu 2000) leading to frequent droughts.

Spatial distribution characteristics of drought disasters in the Hunan Province during the Qing Dynasty

The EOF method was used to decompose the standardized anomaly data from 14 stations in the Hunan Province over 268 years, and the EOF space vector was used as part of the analysis. Due to the complex terrain of the Hunan Province, the spatial distribution of drought disasters is significant and the variability is large. Therefore, the load vector had a slow convergence rate; however, the load vectors still retained the main drought hazard information in each region of the Hunan Province. The significance error test was used to calculate the eigenvalue error range proposed by North et al. (1982). The first four modes passed the test, and the cumulative variance contribution rate was 61.73% (Table 2). The variance contribution rate was more than 7%, which can reflect the situation pertaining to drought disasters in the Hunan Province during the Qing Dynasty. Therefore, the spatial distribution characteristics of the first four modes were analyzed.

The variance contribution rate of the first modal field was 35.22%, which is the most important typical field used for the drought disasters in the Hunan Province. From the spatial distribution of the first modal field (Fig. 3A), it can be observed that the whole region is positive, indicating that there was good spatial agreement, which suggested that the province's drought disasters were largely influenced by regular atmospheric circulation and the other anomalies. The maximum load was distributed in Xiangtan City, indicating that this area had the most serious droughts or the region was characterized by a partial variable rate and was also a sensitive area with regard to drought events.

Table 2 Variance contribution and accumulated variance contribution of the first nine EOF and REOF modes of droughts in the Hunan Province during the Qing Dynasty

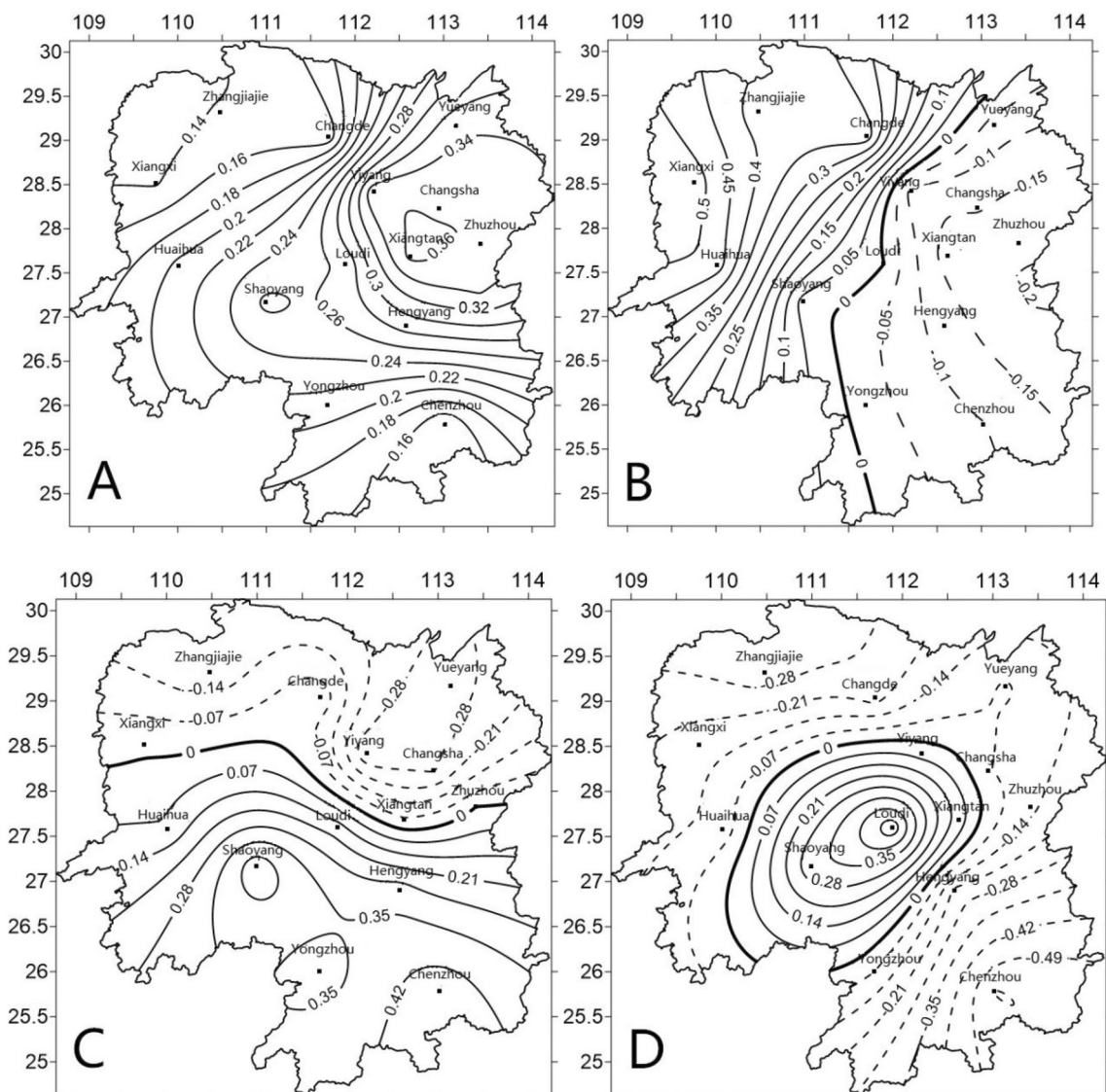| Serial number	EOF		REOF	
	Variance contribution rate (%)	Cumulative variance contribution rate (%)	Variance contribution rate (%)	Cumulative variance contribution rate (%)
1	34.13	34.13	23.78	23.78
2	10.84	44.97	8.30	32.08
3	9.05	54.02	8.40	40.48
4	7.71	61.73	9.13	49.61
5	6.40	68.13	8.59	58.20
6	5.67	73.8	7.27	65.47
7	4.96	78.76	7.24	72.71
8	4.38	83.14	7.20	79.91
9	3.80	86.94	7.03	86.94

Fig. 3 Spatial distribution of the first four EOF modes of drought in the Hunan Province during the Qing Dynasty (**A–D** respectively represent the 1st–4th mode field)

In arid years, the West Pacific subtropical high is weaker and northward, and the South Asian high is stronger and northward. East Asia shows a negative phase distribution of East Asia/Pacific teleconnection from the north to the south. The East Asian subtropical westerly jet is easterly and northward. There is an anticyclone anomaly circulation in the lower-level wind field, south of the Yangtze River. The majority of Hunan is an abnormal divergence region, which results in less precipitation and, consequently, drought.

The second feature field (Fig. 3B) was significantly different from the first feature field, and the contribution to the total variance was 11.76%. This can be expressed as the positive phase located to the east and west of the Yiyang–Loudi–Yongzhou area in Zhuzhou City, while the negative center is located in Huaihua City. Thus, during the Qing Dynasty, droughts in the Hunan Province tended to be alternately serious in eastern and western regions. West heavy (light) and east light (heavy) of the spatial pattern of characteristics, that is, in the eastern part of the drought stress, the west is lighter; on the other hand, when the eastern part of the drought is mild, the western region tends to stress.

From the spatial distribution field of the third mode (Fig. 3C), it can be seen that the drought disasters in the Hunan Province are characterized by a spatial structure spanning in the north–south direction, and the variance contribution rate was 9.83% for Xiangxi, Loudi, and Zhuzhou. Yiyang and Chenzhou showed the maximum positive and maximum negative value, respectively.

From the spatial distribution field of the fourth mode (Fig. 3D), it can be observed that the drought disasters in the Hunan Province during the Qing Dynasty were centered, and the positive center was located in Loudi and Shaoyang. The basin is subject to the effects of topsoil subsidence and a subtropical season, causing the weather to be dry. The dryness is accentuated by the fact that the area is located on the leeward side of Nanling. The area is typically windy (Zhang 2008), with low rainfall resulting in higher drought frequency and intensity.

Spatial abnormal characteristics of drought disasters in the Hunan Province during the Qing Dynasty

Due to the large change of spatiotemporal disasters in the Hunan Province during the Qing Dynasty, the variance contribution rate of the EOF decomposition is not high, the convergence rate is slow, and the abnormal sub-region is complex. In order to further study its regional characteristics, the REOF was carried out on the basis of the EOF decomposition. There are three kinds of methods for determining the number of orthogonal functions of the rotation experience (Wei 1999; Piervitali and Colacino 2001). In this study, the

number of rotation feature vectors were determined by taking the cumulative variance contribution rate of 85% as the standard. Therefore, the vector was rotated, and the distribution of the eigenvector after rotation was relatively uniform (shown in Table 2). According to the principles of rotation main factor analysis, the geographical distribution of the principal load is the important basis for zoning. Using the north significance test, the results showed that the first six modalities through the significance test, drawing the first six main factors of the distribution map, as shown in Fig. 4.

Figure 4 lists the REOF's first six rotational load vectors. The first modal rotational load (RLV1) distribution (Fig. 4A) of the REOF is similar to that of Fig. 3A, but the RLV1 highlights the large area of the northeastern Hunan Province, Yueyang, Yiyang, Changsha, Xiangtan, and Zhuzhou. The load of the site was above 0.68, and throughout the 0.05% significance level test, among them, the center value of Yiyang was as high as 0.858, while the load value of other sites was 0.2 except for Loudi, which can be called as the northeast of the Hunan Province. Due to the low rainfall in the Dongting Lake area, the large amount of evaporation, and the uneven distribution of precipitation times, the water storage capacity was less serious and the water storage capacity was obviously insufficient. The contribution rate of the RLV1 variance was 23.78%, which was the largest of the first six RLV modes (Table 2). Therefore, it was the most common mode of anomalous distribution for the drought disasters in the Hunan Province during the Qing Dynasty.

The results show that the subtropical high is weaker, northerly, and easterly in the northern arid years; the South Asian high and the East Asian subtropical westerly jet are northward, and the lower-level wind field has a large easterly anomaly area in the middle and lower reaches of the Yangtze River. Moreover, the divergence anomaly area is in the north of Hunan, and the convergence anomaly area is in the south, forming the spatial pattern of drought in the north and flood in the south of Hunan.

The second modal rotational load RLV2 (Fig. 4B) is similar to Fig. 3B. The variance contribution rate was 8.30%. The large value area was mainly distributed in Xiangxi and Huaihua in the western Hunan Province, where the load value for Xiangxi was 0.755 for the western part of the western region. This is due to the western region of the Hunan Province which is often subject to the western Pacific subtropical high, the northward rain belt, the end of the rainy season into the summer sunny hot season, high temperatures, and evaporation, causing a high susceptibility to droughts. The magnitude of the third modal rotational load RLV3 (Fig. 4C) was 8.40%. The large value area is mainly located in the southeastern part of the Hunan Province. The large value of the rotational load was in the middle of Chenzhou, 0.873, followed by Hengyang south of the Hunan Province. The contribution rate of the fourth modal rotational load
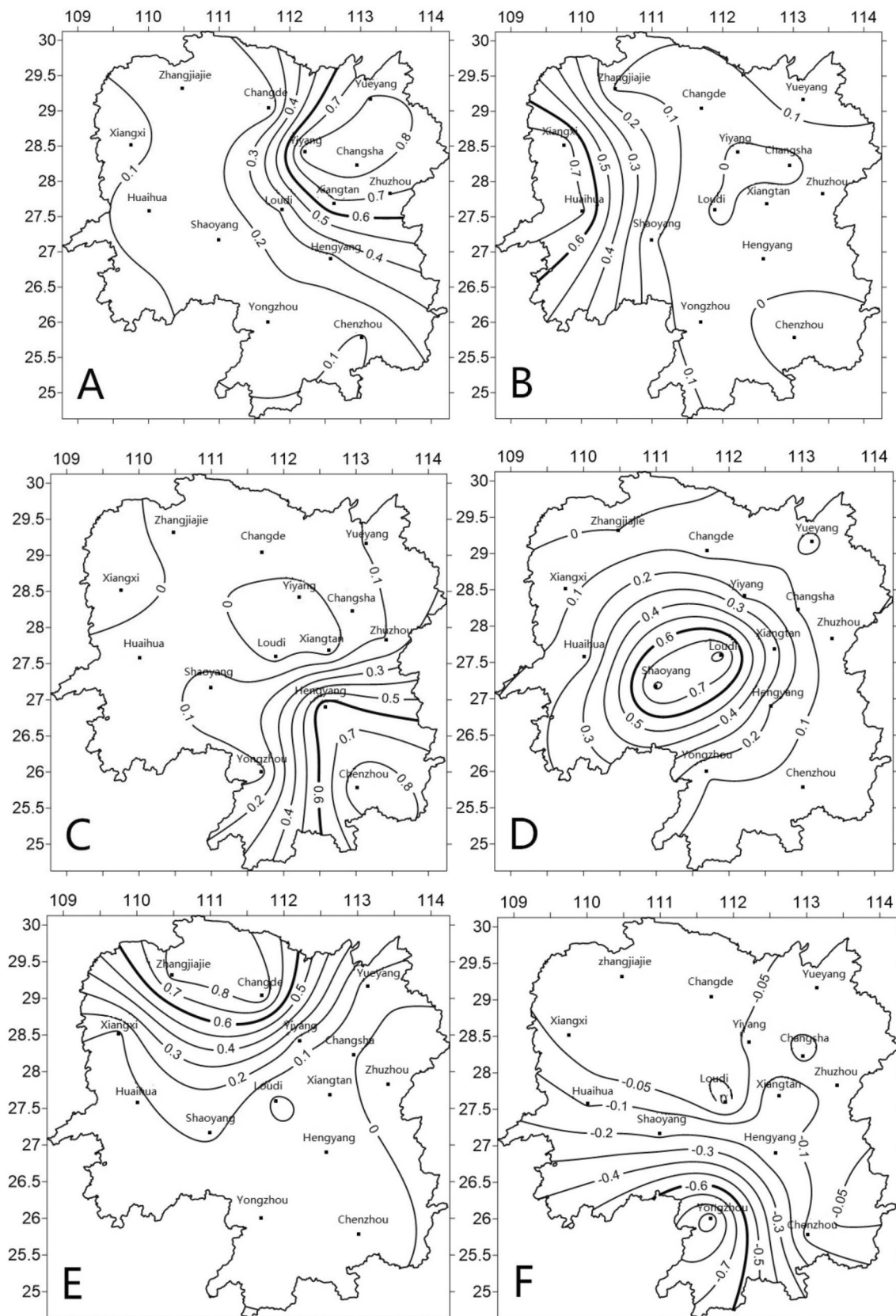
Fig. 4 Spatial distribution of the first six REOF modes of drought in the Hunan Province during the Qing Dynasty (**A–F** respectively represent the 1st–6th mode field)

RLV4 (Fig. 4D) was 9.13%, which clearly highlighted the large area of the central Hunan, and the load of Shaoyang and Loudi was above 0.8.

The fifth modal rotational load RLV5 (Fig. 4E) had a variance contribution rate of 8.59%. The large area is located in Zhangjiajie and Changde, with a load up to 0.871, and is known as the northern part of the type. The variance contribution rate of the sixth modal rotational load RLV6 (Fig. 4F) was 7.27%. The large area is located in Yongzhou, with a load of -0.956.

Discussion

In this study, based on the EOF analysis and the REOF analysis, according to the high load distribution (absolute value ≥ 0.6) of the first six rotational spatial modes, the geographically connected lattice area can be divided into the same drought disaster climate change zone. The high load area covered most of the areas of the Hunan Province, and the adjacent areas are nearly overlapping. The Hunan Province is divided into six arid regions (Fig. 5), namely the northeastern part of the Hunan (I), the western Hunan (II), the southeast Hunan (III), the central Hunan (IV), the northern Hunan (V), and the southwestern Hunan (VI).

Compared with the Hunan Province from 1960 to 2009, the number of dry days in the Hunan Province were divided into five regions (Zhang et al. 2013), namely the Xiangnan, northeastern Hunan, Xiangxi, as well as the climate zonation of five meteorological dry days in the Xiangzhong basin (Fig. 6).

Zhang et al. (2013) obtained five main spatial abnormal climatic regions according to the North criteria. The area with the first rotation mode higher than 0.6 is mainly located in the south of central Hunan, with a variance contribution rate of 25.9%, and the center is located in Chenzhou (0.91). The areas with a second rotation mode higher than 0.6 are mainly distributed in northeast Hunan, with a variance contribution rate of 17.7%, and the center is located in Ningxiang (0.85). The areas with a third rotation mode higher than 0.6 are mainly distributed in northwest Hunan, with a variance contribution rate of 15.5%, and the center is located in Sangzhi (0.92). The areas with a fourth rotation mode higher than 0.4 are mainly distributed in western Hunan, with a variance contribution rate of 9.5%, and the center is located in Huaihua (0.85). The areas with a fifth rotation mode higher than 0.4 are mainly distributed in the Hengyang-Shaoyang basin in central Hunan, with a variance contribution rate of 6.3%, and the center is located in Shaodong (0.68).

In addition to the differences between the western Hunan (II) and the Xiangnan, which is divided into the southeast of Hunan (III) and the southwest of the Hunan (VI) in Fig. 5, the other partition results of the paper are almost the same as those of Zhang Jianming et al.

Conclusions

Based on the drought disaster grade sequence of 14 sites in the Hunan Province from 1644 to 1911, this study focused on the spatial distribution characteristics of drought disasters
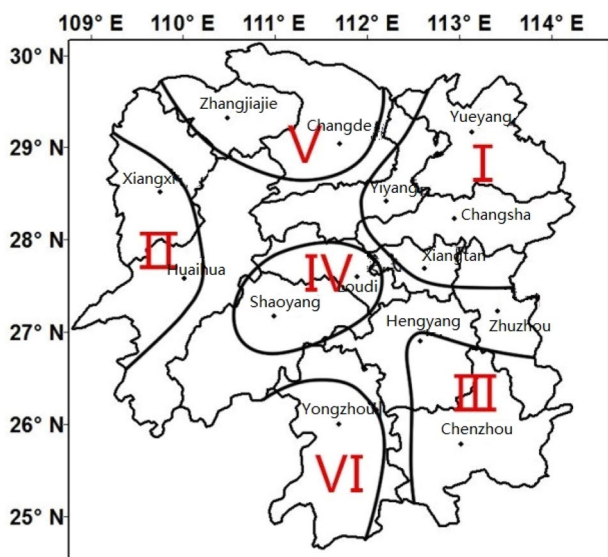

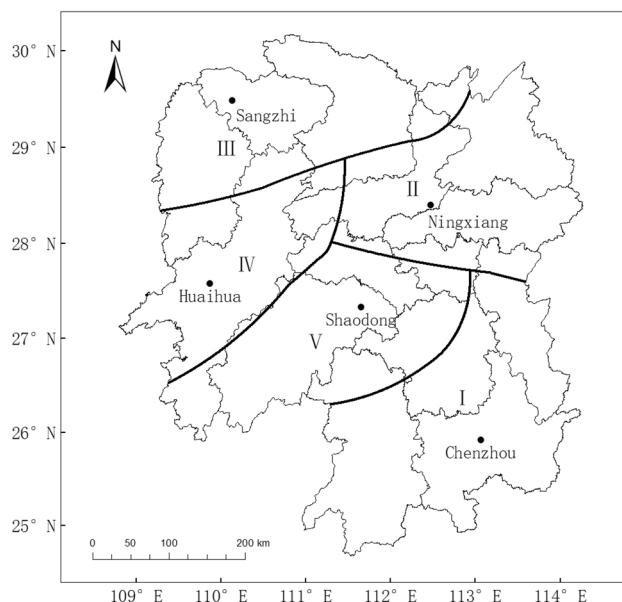**Fig. 5** Six climatic regions of the droughts in the Hunan Province during the Qing Dynasty

Fig. 6 Five climatic regions of the droughts in the Hunan Province (Zhang et al. 2013)

in the Hunan Province of China by using EOF and REOF. The following results were obtained: There were inconsistencies in the number of drought disasters and the intensity of drought disasters in the Hunan Province during the Qing Dynasty. The drought disasters occurred 66.21 times / station, and the drought disasters were the highest in Yongzhou and Chenzhou. The drought intensity was the largest for Shaoyang and Huaihua. The EOF analysis showed that the first four modalities of the drought disasters in the Hunan Province during the Qing Dynasty were 61.73% by the north test, and the first modality was the main characteristic of the drought consistency in the whole region, which showed that the drought disasters in the whole area were generally high, while other typical fields mainly show regional differences in the region, such as the spatial characteristics of the south and north, west and east, center and the opposite of the reverse phase change. Using the results of the REOF, the load value was ≥ 0.60, and the drought disasters in the Hunan Province during the Qing Dynasty can be divided into six regions: Xiangbei (I), western Hunan (II), southeastern Hunan (III) central Hunan (IV), northern Hunan (V), southwestern Hunan (VI).

The study of drought disasters in the Hunan Province of China in Qing Dynasty is of great significance and reference value for disaster prevention, disaster reduction and climate prediction.

The results of this study improve the understanding regarding the spatial characteristics of drought disasters in the Hunan Province during the Qing Dynasty; this will be of significant value in guiding the agricultural production layout and structural adjustment, formulating reasonable drought resistance countermeasures, disaster prevention and mitigation, and providing a scientific basis for the local government and insurance companies to formulate agricultural insurance policies. Furthermore, an in-depth analysis of the spatial characteristics and causes of drought disasters in Hunan can provide useful information for the diagnosis and prediction of drought disasters in this region.

Due to limited data collection and the drought evolution, the temporal and spatial evolution of droughts is influenced by human, economic, and social factors. Climate, topography, landform and vegetation, water conservancy facilities, and human activities can lead to different results. Future studies on the temporal and spatial evolution of droughts will be supported by continuous improvements in data collection and accumulation to increase the accuracy of drought levels in time and space.

Author contributions SB, XQ, and MX conceived and designed the experiments; MX, XQ, and LW performed the experiments; SB, YG, and LW wrote the Chinese manuscript; YG, XQ, and GW translated and polished the manuscript.

Availability of data and material Not applicable.

Code availability Not applicable.

Declarations

Conflict of interest The authors declare that they do not have any commercial or associative interest that represents a conflict of interest in connection with the paper they submitted.

References

Achour Y, Pourghasemi HR (2020) How do machine learning techniques help in increasing accuracy of landslide susceptibility maps? Geosci Front 11(3):871–883

Chen JY, Wang KY (2010) Records of Xiang Tan. Yuelu Press, Hunan

Chen YY, Chen N, Wang SG, Qian ZA, Mu JH (2010) Temporal and spatial change features of precipitation over China-Mongolia arid-and semiarid-areas (I): Annual Rainfall Feature and May~September One REOF analyses. Plat Meteorol 29(1):33–43

Chinese Academy of Meteorological Sciences (1981) A collection of drought and flood in china in recent five years. China Cartographic Publishing House, Beijing

Du J, Fang J, Xu W, Shi P (2013) Analysis of dry/wet conditions using the standardized precipitation index and its potential usefulness for drought/flood monitoring in Hunan Province, China. Stoch Environ Res Risk Assess 27:377–387

Findell KL, Delworth TL (2010) Impact of common sea surface temperature anomalies on global drought and pluvial frequency. J Clim 23:485–503

Gao C, Zou WQ (2013) An analysis of temporal and spatial characteristics of the drought disasters in Fenhe River Basin in Ming Dynasty. J Shanxi Univ 36(1):21–26

Guo R, Zhu Y, Liu Y (2020) A comparison study of precipitation in the Poyang and the Dongting Lake basins from 1960–2015. Sci Rep 10:3381

Huang ZZ, Zhang ZN, Deng XH (2009) Records of Bao Qing. Yuelu Press, Hunan

Li YP, Chen CC, Zhang YQ, Bi SB (2015) Spatial temporal characteristics of drought disasters in Henan Province in Ming Dynasty. J Arid Land Resour Environ 29(5):174–179

Liu XG (2000) Characteristics and countermeasures of drought in Hunan Province. Chin Water Resour 5:43

Luo B, Zhang C (2010) Relations between drought and flood in dominant flood season in Hunan and circulation characteristic and sea surface temperature in spring. Plateau Meteorol 29(5):1322–1330

Luo B, Huang W, Shuai X, Xie B, Peng L (2009) Study on drought risk regionalization of rice production in Hunan Province. J Anhui Agric Sci 37(33):16429–16431

Mi HB, Tan GR, Qing XT (2016) Analysis of summer drought events in Xiangxi of Hunan Province. Trans Atmos Sci 39(1):102–109

National Science and Technology Commission (1990) Climate China Science and Technology Blue Book, no. 5. Science and Technical Documentation Press, Beijing

North GR, Bell TL, Cahalan RF, Moeng FJ (1982) Sampling errors in the estimation of empirical orthogonal function. Mon Weather Rev 110(2):699–706

Piervitali E, Colacino M (2001) Evidence of drought in Western Sicily during the period 1565–1915 from Liturgical Offices. Clim Change 49(1/2):225–238

Shi N (2002) Multivariate analysis method in meteorological research and forecast. China Meteorological Press, Beijing

Ummenhofer CC, Sen GA, Briggs PR, England MH, McIntosh PC, Meyers GA, Pook MJ, Raupach MR, Risbey JS (2011) Indian and Pacific Ocean influences on Southeast Australian drought and soil moisture. J Clim 24:1313–1336

Wei FY (1999) Modern climate statistics diagnosis and prediction technology. China Meteorological Press, Beijing

Wen KG, Jiang HR (2007) China Meteorological Disaster Ceremony. China Meteorological Press, Beijing

Wen KG, Zeng QH (2006) China Meteorological Disaster. China Meteorological Press, Beijing

Xie L, Zhu Y (2005) Analysis on the causes of frequent floods and droughts in Hunan Province. Hunan Water Conserv Hydropower 5(11–12):35

Xing S, Zhao JB (2011) The research on drought disasters and wavelet analysis in Jinan in Ming Dynasty. J Earth Environ 2(5):619–624

Xu XC, Ge QS, Zheng JY, Dai EB, Liu CW (2011) Drought risk assessment on regional agriculture: a case in southwest China. Prog Geol 30(7):883–890

Yang S, Xu L (1994) Linkage between Eurasian Winter Snow Cover and Chinese Summer Rainfall: different from the Snow-Indian Monsoon Circulation. Int J Climatol 14:739–750

Yang ZR, Zhang WM (1994) Distribution law in time and space of historical drought of Hunan Province. J Catastrophol 9(2):32–37

Yin JK, Yu DY, Wu WT (1997) Research on natural disasters in Beijing. China Environmental Science Press, Beijing

Zhang DE (2004) China's 3000 years meteorological records. Education Publishing House, Jiangsu

Zhang JM, Li ZX, Zhang XP, Zhang J, Shao ZF (2009) A fuzzy evaluation of the regional drought in Hunan Province. Prog Geo 28(4):629–635

Zhang JM, Liao YF, Peng JD, Zhou JJ (2013) Spatial and Temporal variation of meteorological drought days in Hunan Province. Chin J Agrometeorol 34(6):621–628

Zhang J, Liao Y, Wu H, Zhang J, Zhao H (2018) Characteristics of atmospheric circulation anomalies and drought in summer and autumn in Hunan Province. J Arid Meteorol 36(3):353–364

Zhang X, Chen N, Sheng H, Ip C, Yang L, Chen Y, Bueti C (2019) Urban drought challenge to 2030 sustainable development goals. Sci Tot Environ 693:133536

Zhang JM (2008) The Spatio-temporal distribution of drought in Hunan Province in past 36 years. Climate Center of Hunan Province, Hunan, pp 1–76

Zhao Y, Shi JF, Shi SY, Yu J, Lu H (2017) Tree-ring latewood width based July–August SPEI reconstruction in South China since 1888 and its possible connection with ENSO. J Meteor Res 31(1):39–48